Bandwidth Enhancement of an Inverted F-Shape Notch Loaded Rectangular Microstrip Patch Antenna for Wireless Applications in L and S-band

Ramesh Kumar Verma[1] (ORCID)

Abstract

This article presents a compact antenna design of overall size 38.4 mm × 46.8 mm having square shape and an inverted F-shape notches. The proposed antenna of single band is resonating between 1.69 and 2.91 GHz at two frequencies 1.98 GHz and 2.56 GHz. The proposed structure of antenna design has three square shape notches at corner and an inverted F-shape notch. The loading of notches inside radiating patch increases the effective current path. Due to increase of current path, radiation of antenna increases and large bandwidth is obtained. The reflection coefficient and impedance bandwidth both are increases gradually by loading different notches in radiating patch. Parametric investigation is also performed to figure out the effect of different parameters. The proposed antenna shows fractional bandwidth of 53.04% (1220 MHz) resonating at frequencies 1.98 GHz and 2.56 GHz with good reflection coefficient of − 27.14 dB and − 21.49 dB respectively. To validate the antenna performance, the simulated results for the proposed antenna are compared with measurements taken with fabricated antenna. The operating frequency band of proposed antenna is useful in L and S-band for PCS (1.85–1.99 GHz), UMTS (1.92–2.17 GHz), WLAN (2.4–2.484 GHz), and WiMAX (2.5–2.69 GHz). A stable peak gain of 2.9–3.84 dB and antenna efficiency of 81–91% is observed in entire resonating band.

Keywords Compact · Notches · F-shape notch · Bandwidth · WLAN · WiMAX · IE3D

1 Introduction

Compact and low-profile antennas with extensive resonant bandwidth and consistent gain are in higher demand as a result of wireless communication devices. The microstrip antenna (MSA) offers a number of advantages, including light weight, low profile and compactness, but it also has a number of drawbacks, including narrow bandwidth, low efficiency, spurious radiation at the feed and reduced gain [1]. For MSA design, a variety of substrates with dielectric constants ranging from 2.2 to 12 can be employed

✉ Ramesh Kumar Verma
  ramesh85.ec@gmail.com

1 Department of Electronics and Communication Engineering, Bundelkhand Institute of Engineering and Technology, Jhansi, UP, India

[2]. High bandwidth and efficiency are provided by substrates with a lower dielectric constant. MSA can have a wide impedance bandwidth by employing a variety of strategies, such as evaluating various patch shapes and loading various types of notch and slots in radiating patch.

To improve the performance of antenna along with bandwidth enhancement, different types of antenna design using different technique has been presented. Liu et al. [3] presented a large size of $200 \times 130 \text{mm}^2$ patch antenna for bandwidth improvement of 13% (260 MHz) between frequency ranges 1.88 GHz to 2.14 GHz using differential feed while a fractal antenna of size $40 \times 40 \text{mm}^2$ is proposed by Gangwar et al. [4] with one hexagonal and six circular shape slots showing bandwidth of 45.16% and 2.6 dB gain. However, Gupta et al. [5] also presented an optimized fractal antenna design of size $51 \times 59 \text{mm}^2$ using PSO along with hybrid bacterial foraging (BF) exhibiting 34% impedance bandwidth. Geetharamani and Aathmanesan [6] presented a metamaterial based antenna of size $30 \times 40 \text{mm}^2$ with FR-4 (Glass epoxy) substrate for 2.4 GHz exhibiting impedance bandwidth of 574 MHz and 3.23 dB gain using split ring at back side of structure. In [7], Cheng and Yao presented a wideband dipole antenna of compact size with enhanced bandwidth of 51.4% (750 MHz) using narrow cross shaped magneto-electric dipole for GNSS/GPS applications while Verma and Srivastava designed an inverted T-shaped slot [8] loaded antenna of size $38.43 \times 46.86 \text{mm}^2$ having fractional bandwidth of 48.25% (1179 MHz) at 2.477 GHz and plus shaped slot [9] loaded antenna of size $39 \times 47.6 \text{mm}^2$ with fractional bandwidth of 48.68% (1155 MHz) at 2.391 GHz. Gupta and Chaudhary [10] also designed a metamaterial based compact antenna of size $48 \times 24 \text{mm}^2$ with stub loaded resonating between 1.67 and 2.76 GHz having bandwidth of 49.2% (1090 MHz).

Apart from these antennas, Deshmukh and Ray [11] also presented an antenna structure of very large size $51 \times 110 \text{mm}^2$ for GSM application with L-shapes slot having bandwidth of 28% (290 MHz) while Gupta et al. [12] proposed a flower shape wideband with reduced ground antenna of large size $55 \times 64 \text{mm}^2$ resonating at 1.975 GHz between frequency ranges 1.49–2.46 GHz with impedance bandwidth of 49% (970 MHz). In [13], Ansari et al. presented a disk shape of single and multi layered antenna of size $88 \times 62 \text{mm}^2$ with impedance bandwidth of 36.5% (985 MHz) at 3 GHz resonant frequency for WLAN and WiMAX applications while Kamakshi et al. [14] designed a novel antenna of size $120 \times 80 \text{mm}^2$ using notch and slot with bandwidth of 30.5% (560 MHz) at 1.84 GHz. Furthermore, a U-slot antenna with dual feed of very size $76.8 \times 76.8 \text{mm}^2$ resonating between 1.09 and 1.51 GHz with 32.1% (420 MHz) bandwidth is presented by He et al. [15]. Zhou et al. [16] proposed a wideband dipole antenna of very large size $106 \times 106 \text{mm}^2$ with cross-shaped slot providing bandwidth of 48% (1070 MHz) using radiator, director and coupler while Sun et al. [17] also described a wideband and compact antenna design of very large size $100 \times 100 \text{mm}^2$ for bandwidth increment of 32% (500 MHz) using shorting load. Moreover, a dual mode with stub loaded endfire wideband antenna structure of size $88 \times 88 \text{mm}^2$ with semicircular radiator offering bandwidth of 24.8% (650 MHz) at 2.45 GHz is designed by Zhang et al. [18]. Bala et al. [19] designed a metamaterial based antenna structure of overall size $40 \times 48 \text{mm}^2$ resonating at 2.73 GHz with 41% (1118 MHz) impedance bandwidth. Additionally, Sharma et al. [20] presented an antenna design of size $60 \times 60 \text{mm}^2$ with π-shape slot resonating between 2.32 and 3.35 GHz having bandwidth of 40.23% (1130 MHz). In [21], Chaturvedi and Raghavan presented a compact metamaterial based antenna of size $30 \times 17 \text{mm}^2$ using L-shape stub and split ring resonator operated at 2.45 GHz with poor gain of 1.86 dB and 19.4% (480 MHz) bandwidth. However, Dwivedi et at. [22] proposed a two port MIMO antenna of size $37 \times 30 \text{mm}^2$ with

circular polarization exhibiting 900 MHz impedance bandwidth for 5G applications. In the above reported antennas, all of them have limitations of narrow bandwidth and some have large size and complex design compared to proposed antenna.

In this paper, the impedance bandwidth of microstrip antenna is increased by loading three square shape notches of same size and an inverted F-shape notch inside antenna patch. The above reported antenna design of single band in the literature part, most of them are not increased the impedance bandwidth beyond 1000 MHz, but proposed antenna offers fractional bandwidth of 53.04% (1220 MHz) between range 1.69–2.91 GHz resonating at two frequencies 1.98 GHz and 2.56 GHz in L and S-band. The operating range of proposed antenna is suitable for PCS (1.85–1.99 GHz), UMTS (1.92–2.17 GHz) [23], WLAN (2.4–2.484 GHz) and WiMAX (2.5–2.69 GHz) [24]. The proposed antenna is simulated and analysed by using IE3D [25] simulation software.

The content of the paper is organized in the following sections. The design parameters and geometry of proposed antenna are presented in Sects. 2 and 3 while step by step design process along with simulation and parametric study of the proposed antenna are discussed in Sects. 4 and 5. In Sects. 6 and 7, results discussion and experimental validation along with performance comparison of proposed antenna with pervious published work are discussed. Finally, the conclusion is described in last Sect. 8.

2 Antenna Design Parameters of Proposed Structure

For calculating the physical size of antenna, the parameters like design frequency (2.45 GHz), substrate thickness (1.6 mm), loss tangent (0.02) and dielectric constant (4.4) are used. For rectangular MSA design, the length (L_p) and width (W_p) of antenna patch is calculated by using equations presented in [2]. The Eqs. (1)–(4) can be used to determine width and length of antenna patch.

$$W = \frac{c}{2f_r} \sqrt{\frac{2}{\varepsilon_r + 1}}$$
(1)

where W is width of patch, f_r is design frequency of antenna, ε_r is dielectric constant of substrate and $c = 3 \times 10^8$ m/s (speed of light).

$$\varepsilon_{\text{reff}} = \frac{\varepsilon_r + 1}{2} + \frac{\varepsilon_r - 1}{2}\left(1 + \frac{12h}{W}\right)^{-\frac{1}{2}}$$
(2)

where h is thickness (1.6 mm) of substrate and $\varepsilon_{\text{reff}}$ is effective dielectric constant.

$$\Delta L = 0.412 \times h \times \frac{(\varepsilon_{reff} + 0.30)(\frac{W}{h} + 0.264)}{(\varepsilon_{reff} - 0.258)(\frac{W}{h} + 0.8)}$$
(3)

where ΔL represents extension length.

$$L = \frac{c}{2f_{r_{\sqrt{\varepsilon_{reff}}}}} - 2(\Delta L)$$
(4)

where L represents actual length of patch.

The size of ground plane can be determined by Eqs. (5) and (6) [26].

$$Lg = L + 6h \tag{5}$$

$$Wg = W + 6h \tag{6}$$

The length and width of the patch is obtained 28.8 mm and 37.2 mm whereas ground plane length and width is obtained 38.4 mm and 46.8 mm respectively.

3 Proposed Antenna Geometry

The structure of proposed antenna with dimentional parameters are shown in Fig. 1a, b. The compact patch of size 28.8 mm×37.2 mm at frequency 2.45 GHz is designed with ground plane of size 38.4 mm×46.8 mm. The proposed antenna design has three square shape notches of size 5 mm×5 mm each at three corner. An inverted F-shape notch has been loaded at top of patch having vertical arm of size 20 mm×5 mm and two horizontal arms of size 5 mm×5 mm and 7 mm×5 mm. The loading of notches inside radiating patch, increases the effective current path and surface current distribution is also changed. Due to increase of current path, radiation of antenna increases and large bandwidth is obtained. A microstrip line feed of 50Ω is connected at remaining corner (left lower edge) of radiating patch with feed strip of length 2.4 mm and width 5 mm at coordinate (2.4, 7.3).
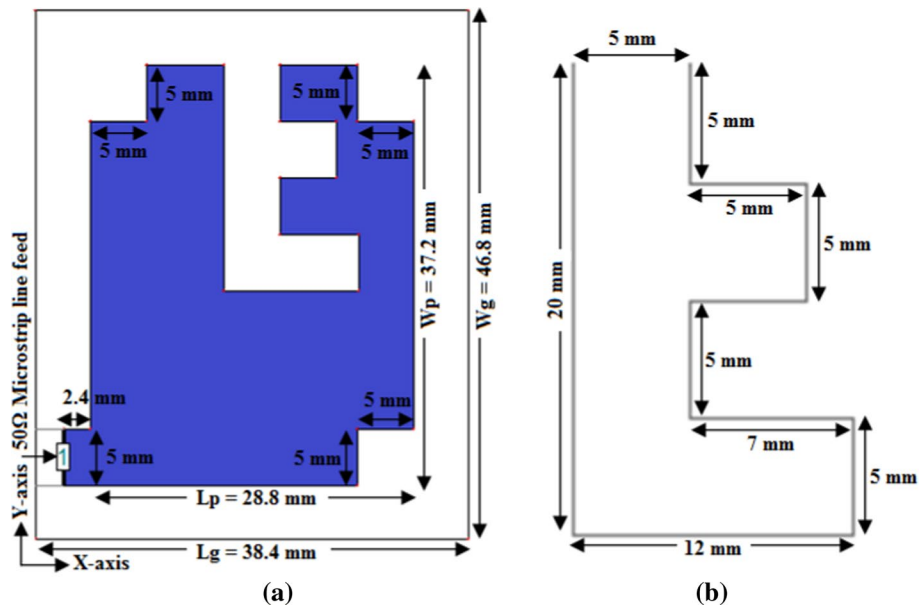

Fig. 1 Geometry of proposed antenna **a** Top view, **b** Inverted F-shape design

4 Antenna Design Process and Simulation

Flow chart for antenna design procedure is shown in Fig. 2 whereas Fig. 3 shows the step by step designing and simulation of antenna-1 (conventional) to antenna-5 (proposed). All designed antennas (Antenna-1 to Antenna-5) are simulated between frequency ranges 1 GHz to 3 GHz. Initially, antenna-1 (conventional) is designed at calculated size of ground and patch with 50Ω line feed connected by strip of size 2.4 mm×5 mm. The conventional antenna (Antenna-1) is resonating between 2.21 and 2.36 GHz at resonant frequency 2.29 GHz. A narrow bandwidth of only 6.56% (150 MHz) is achieved with poor reflection coefficient of − 10.41 dB at frequency 2.29 GHz. The geometry and reflection coefficient plot of antenna-1 (conventional) is shown in Figs. 3a and 4 respectively.

In next step, notch loaded antenna (Antenna-2) is designed by loading three square shape notches of same size 5 mm×5 mm each at three corners of patch as shown in Fig. 3b. The notches loaded antenna (Antenna-2) is resonating between 2.24 and 2.43 GHz at resonant frequency 2.34 GHz. The bandwidth of 8.16% (190 MHz) is achieved with poor reflection coefficient of − 10.41 dB. The reflection coefficient plot of notches loaded antenna-2 is shown in Fig. 4. It can noticed that there is no incerement in reflection coefficient but small increment in bandwidth is obtained by loading three square shape notches.

For further improvement in bandwidth and reflection coefficient, antenna-3 is designed by loading a vertical notch of size 20 mm×5 mm at the top edge of radiating patch symmetrically at coordinate (19.21, 32.06) as shown in Fig. 3c. The characteristic of this antenna is changed in dual band and antenna is resonating at frequencies 1.79 GHz and 2.72 GHz with reflection coefficient of − 14.89 dB and − 14.18 dB respectively. The
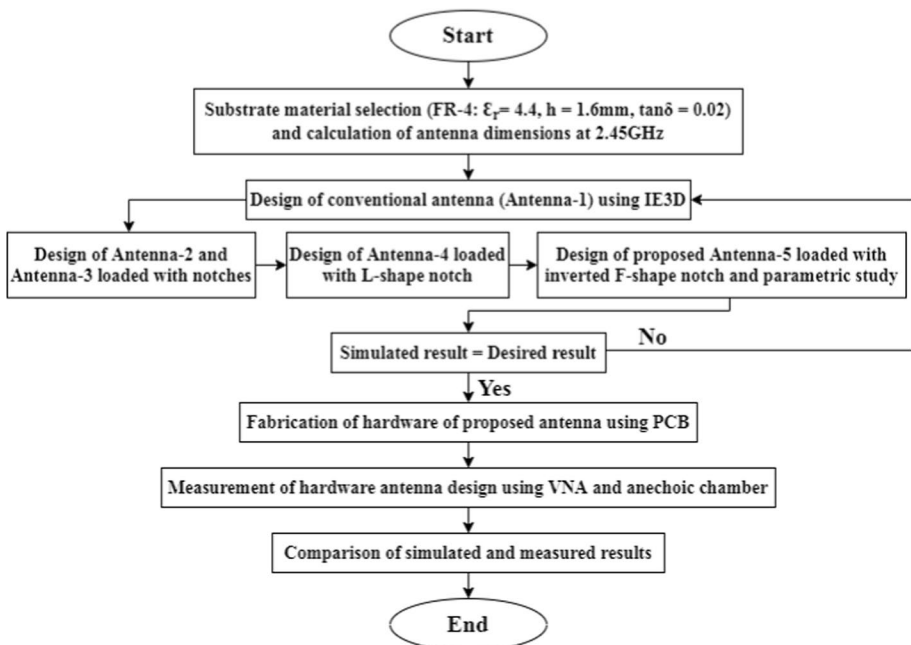

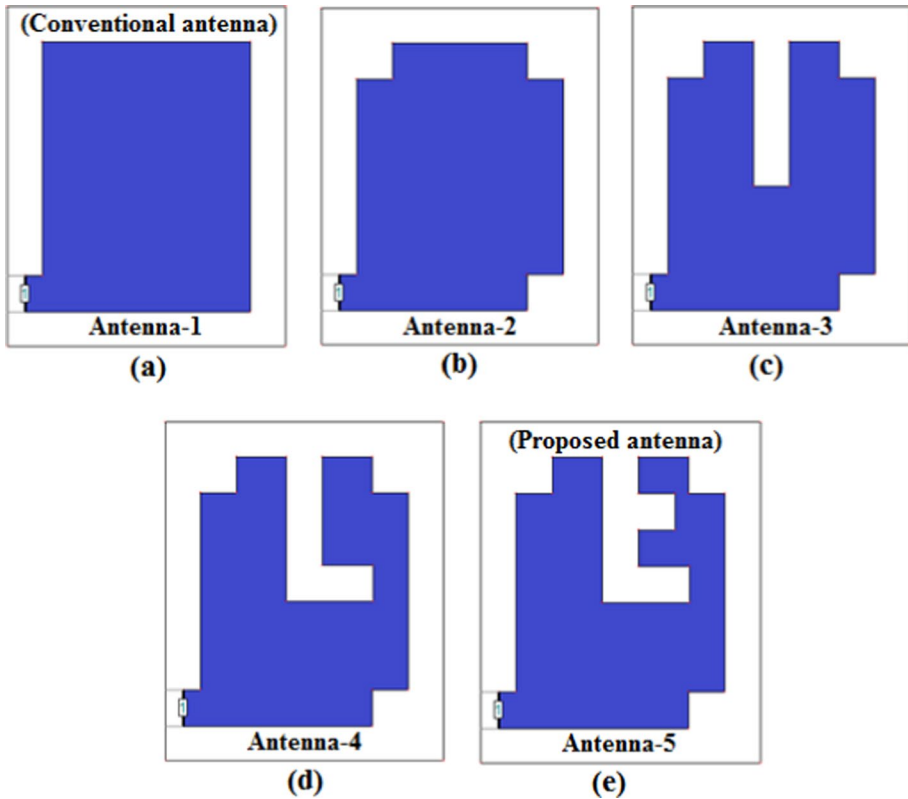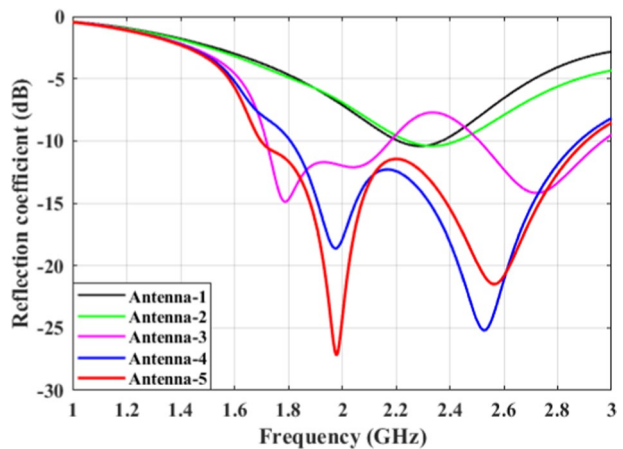**Fig. 2** Flow chart of antenna design procedure

Fig. 3 Step by step geometry of proposed antenna

Fig. 4 Reflection coefficient plot of inverted F-shape notch loaded antenna-5 (proposed) with antenna-1, antenna-2, antenna-3 and antenna-4

bandwidth of 23.59% (460 MHz) in lower band between 1.72 and 2.18 GHz and bandwidth of 16.79% (460 MHz) in higher band between 2.51 and 2.97 GHz is obtained. It can noticed that reflection coefficient and bandwidth both are increased by loading vertical

notch in antenna patch. The reflection coefficient plot of vertical notch loaded antenna-3 is shown in Fig. 4.

In next step, L-shape notch loaded antenna (antenna-4) is designed by loading a rectangular shape slot of size 7 mm × 5 mm in pervious notch of antenna-3 as shown in Fig. 3d. Further, the behaviour of L-shape notch loaded antenna-4 changed into single band but it resonates at two frequencies. This antenna is resonating between 1.81 and 2.88 GHz with improved bandwidth of 45.63% (1070 MHz). The improved reflection coefficient of − 18.62 dB and − 25.19 dB is observed at two frequencies 1.98 GHz and 2.53 GHz respectively. The reflection coefficient plot of L-shape notch loaded antenna-4 is shown in Fig. 4.

Finally, an inverted F-shape notch loaded antenna-5 (proposed) is designed by loading another square shape slot of size 5 mm × 5 mm in pervious L-shape notch loaded antenna-4 as shown in Fig. 3e The bandwidth of antenna-5 is obtained 53.04% (1220 MHz) resonating between 1.69 and 2.91 GHz with good reflection coefficient of − 27.14 dB and − 21.49 dB at frequencies 1.98 GHz and 2.56 GHz respectively. It can notice that the inverted F-shape notch loaded antenna resonates with improved bandwidth and reflection coefficient both. The reflection coefficient graph of inverted F-shape notch loaded antenna (antenna-5) is shown in Fig. 4 while performance comparison of inverted F-shape notch loaded antenna (antenna-5) with antenna-1, antenna-2, antenna-3 and antenna-4 is shown in Table 1.

5 Parametric Study

The parametric study is performed for both lower and upper horizontal arm of inverted F-shape notch loaded antenna-5. The lower horizontal arm of size 7 mm × 5 mm is investigated at 3 mm × 5 mm, 5 mm × 5 mm, 7 mm × 5 mm, 9 mm × 5 mm and 11 mm × 5 mm with 2 mm variation while upper horizontal arm of size 5 mm × 5 mm is investigated at 3 mm × 5 mm, 4 mm × 5 mm, 5 mm × 5 mm and 6 mm × 5 mm with 1 mm variation.

In case of lower horizontal arm variations, the dual band with bandwidth of 27.7% (540 MHz) in lower band between 1.68 and 2.22 GHz and 24.43% (640 MHz) in higher band between 2.30 and 2.94 GHz are achieved at size 3 mm × 5 mm with reflection coefficient of − 24.21 dB and − 17.63 dB at frequency 1.76 GHz and 2.63 GHz while single band with bandwidth of 48.39% (1130 MHz) between 1.77 and 2.90 GHz with

Table 1 Performance compression of antenna-1, antenna-2, antenna-3, antenna-4 and antenna-5

Antennas	Lower freq. (GHz)	Higher freq. (GHz)	Reflection coefficient (dB)	Resonant freq. (GHz)	VSWR	Bandwidth (%)
Antenna-1	2.21	2.36	− 10.41	2.29	1.86	6.56 (150 MHz)
Antenna-2	2.24	2.43	− 10.41	2.34	1.86	8.16 (190 MHz)
Antenna-3	1.72	2.18	− 14.89	1.79	1.45	23.59 (460 MHz)
	2.51	2.97	− 14.18	2.72	1.49	16.79 (460 MHz)
Antenna-4	1.81	2.88	− 18.62	1.98	1.27	45.63 (1070 MHz)
			− 25.19	2.53	1.12	
Antenna-5 (proposed)	1.69	2.91	− 27.14	1.98	1.09	53.04 (1220 MHz)
			− 21.49	2.56	1.18	

reflection coefficient of − 22.28 dB and − 22.4 dB at frequency 1.98 GHz and 2.55 GHz respectively for size 5 mm×5 mm, 53.04% (1220 MHz) between 1.69 and 2.91 GHz with reflection coefficient of − 27.14 dB and − 21.49 dB at frequency 1.98 GHz and 2.56 GHz respectively for size 7 mm×5 mm, 45.44% (1070 MHz) between 1.82 and 2.89 GHz with reflection coefficient of − 17.24 dB and − 24.5 dB at frequency 1.97 GHz and 2.54 GHz respectively for size 9 mm×5 mm and 43.37% (1030 MHz) between 1.86 and 2.89 GHz with reflection coefficient of − 13.89 dB and -26.58 dB at frequency 1.96 GHz and 2.53 GHz respectively for size 11 mm×5 mm is achieved. The variation in reflection coefficient at different size of lower horizontal arm is shown in Fig. 5. Out of above five variations, maximum bandwidth of 53.04% (1220 MHz) with good reflection coefficient of − 27.14 dB and − 21.49 dB is achieved at size 7 mm×5 mm.

In case of upper horizontal arm variations, the dual band behaviour is achieved for size 3 mm×5 mm while single band behaviour is achieved for sizes 4 mm×5 mm, 5 mm×5 mm and 6 mm×5 mm. The dual band with bandwidth of 25.91% (500 MHz) in lower band between 1.68 and 2.18 GHz and 21.88% (570 MHz) in higher band between 2.32 and 2.89 GHz are achieved at size 3 mm×5 mm with reflection coefficient of − 20.19 dB and -16.91 dB at frequency 1.99 GHz and 2.61 GHz while single band with bandwidth of 46.81% (1100 MHz) between 1.80 and 2.90 GHz with reflection coefficient of − 19.43 dB and − 23.39 dB at frequency 1.97 GHz and 2.55 GHz respectively for size 4 mm×5 mm, 53.04% (1220 MHz) between 1.69 and 2.91 GHz with reflection coefficient of − 27.14 dB and − 21.49 dB at frequency 1.98 GHz and 2.56 GHz respectively for size 5 mm×5 mm and 44.40% (1050 MHz) between 1.84 and 2.89 GHz with reflection coefficient of − 15.46 dB and − 25.72 dB at frequency 1.97 GHz and 2.53 GHz respectively for size 6 mm×5 mm is achieved. Out of above four variations, maximum bandwidth of 53.04% (1220 MHz) with good reflection coefficient of − 27.14 dB and− -21.49 dB is achieved at size 5 mm×5 mm. The variation in reflection coefficient at different size of upper horizontal arm is shown in Fig. 6.

Fig. 5 Reflection coefficient plot at 3 mm×5 mm, 5 mm×5 mm, 7 mm×5 mm, 9 mm×5 mm and 11 mm×5 mm
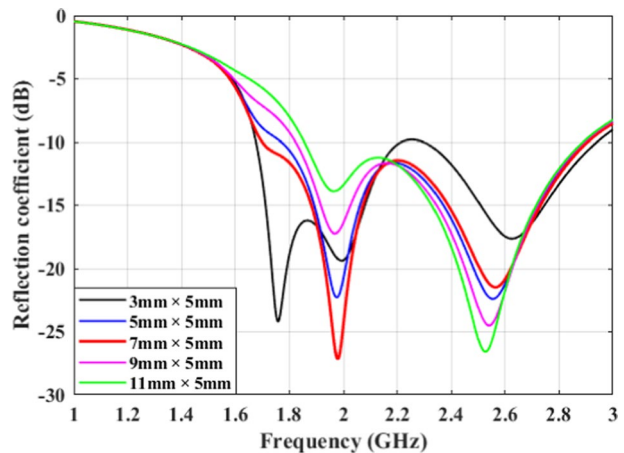
Fig. 6 Reflection coefficient plot at 3 mm×5 mm, 4 mm×5 mm, 5 mm×5 mm and 6 mm×5 mm
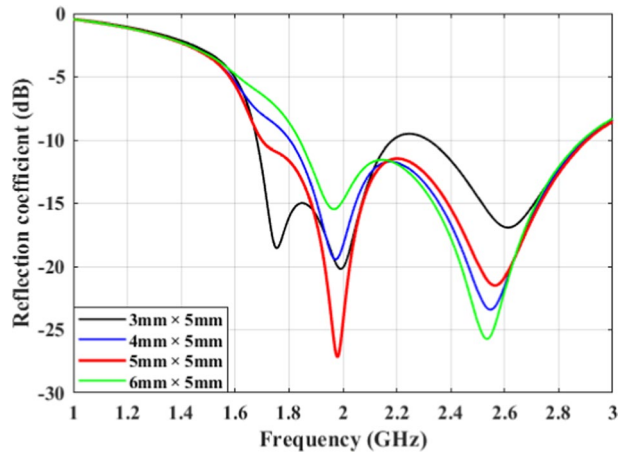

6 Results and Discussion

The performance of inverted F-shape notch loaded antenna is investigated between 1.69 and 2.91 GHz resonating band using IE3D tool. Reflection coefficient and VSWR plot of proposed antenna is shown in Fig. 7. The proposed antenna is resonating at two frequencies in single band characteristic. The obtained bandwidth of proposed antenna is 53.04% (1220 MHz) resonating at 1.98 GHz and 2.56 GHz with good reflection coefficient of − 27.14 dB and − 21.49 dB respectively. VSWR of antenna lies below 2 and its value is 1.09 and 1.18 at resonant frequencies 1.98 GHz and 2.56 GHz respectively.

Figure 8 shows the distribution of current density at frequencies 1.98 GHz and 2.56 GHz. The radiation mechanism of an antenna is described by direction and strength of surface current density in the patch. The proposed antenna is linearly polarized. The maximum current density at frequencies 1.98 GHz and 2.56 GHz is 293A/m and 165A/m respectively. At lower resonating frequency 1.98 GHz, the density of surface current is maximum near left edge of radiating patch as well as lower arm of inverted F-shape notch while it is increases near lower edge of radiating patch and around both arm of inverted F-shape notch at upper resonating frequency 2.56 GHz.

Fig. 7 Simulated reflection coefficient and VSWR plot of proposed antenna
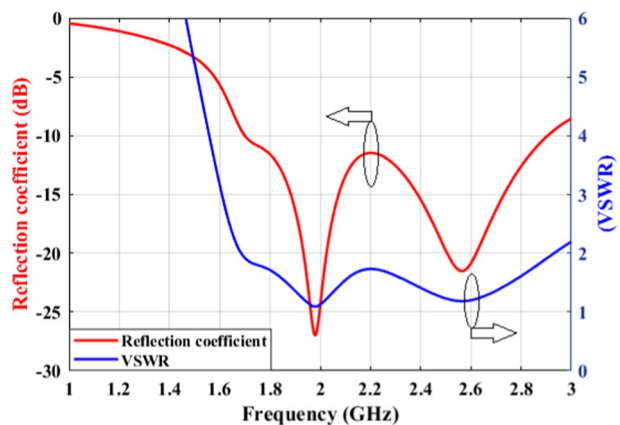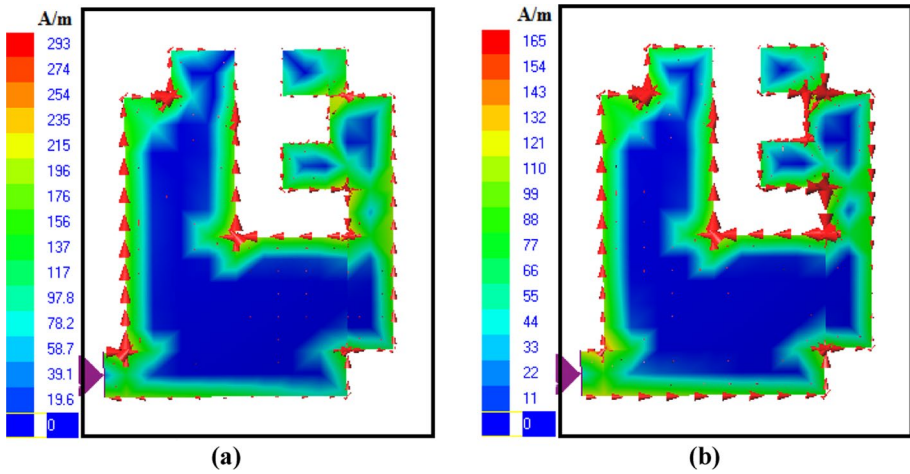
**Fig. 8** Surface current density at frequencies **a** 1.98 GHz **b** 2.56 GHz

The input impedance Z plot (real and imaginary) of proposed antenna is shown in Fig. 9. The value of input impedance Z is 50.68 + j4.38Ω at frequency 1.98 GHz while it is 51.78 + j8.42Ω at frequency 2.56 GHz. The antenna is excited with 50Ω characteristic impedance using line feed while magnitude of input impedance is |Z|= 50.86Ω at frequency 1.98 GHz and |Z|= 52.46Ω at frequency 2.56 GHz. Hence, good impedance matching is obtained and only mismatch of 0.86Ω and 2.46Ω is occurred at frequencies 1.98 GHz and 2.56 GHz respectively.

7 Experimental Results and Validation

To validate the geometry of proposed antenna, a prototype antenna is fabricated using FR-4 substrate (glass epoxy) of thickness 1.6 mm. Front view and back view of fabricated hardware antenna is shown in Fig. 10a, b respectively. The measured bandwidth is achieved

**Fig. 9** Z parameter graph (real and imaginary) of proposed antenna

(a) **(b)**
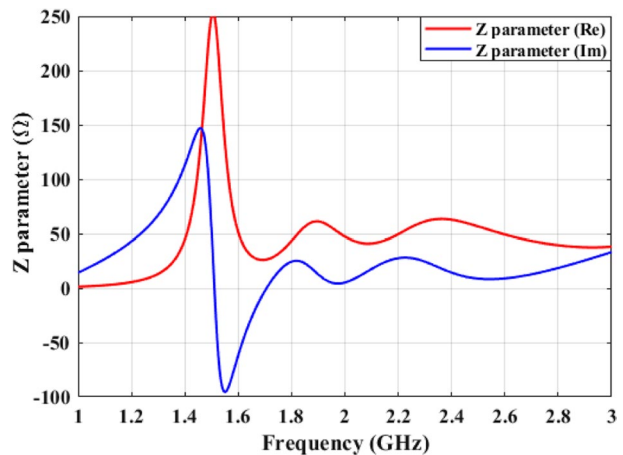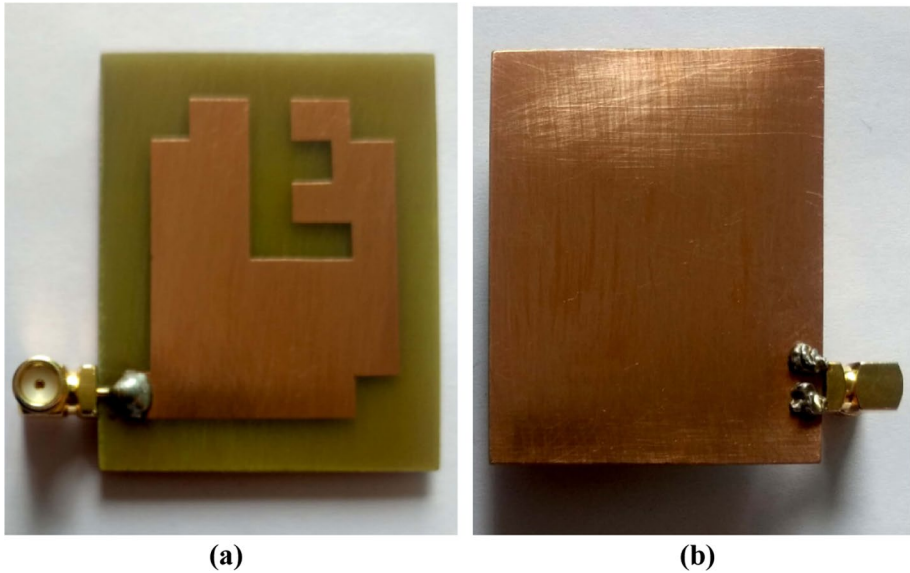
Fig. 10 Hardware design of proposed antenna **a** Front view **b** Back view

43.12% (940 MHz) between 1.71 and 2.65 GHz resonating at frequencies 1.97 GHz and 2.55 GHz with − 20.65 dB and − 25.29 dB reflection coefficient measured by vector network analyzer (VNA) between 1 to 3 GHz for 201 frequency points. The simulated and measured reflection coefficient plot and comparative performance of proposed antenna is shown in Fig. 11 and Table 2 respectively. The photograph of measured reflection coefficient and measurement setup is shown in Fig. 12a, b respectively. A small difference of 280 MHz in bandwidth and 10 MHz in resonant frequency is obtained in measured and simulated antennas due to error occurred in etching process and soldering of line feed connector.

Figure 13a, b shows the E-plane and H-plane radiation patterns (simulated and measured) of proposed antenna at frequencies 1.98 GHz and 2.56 GHz measured in an anechoic

Fig. 11 Simulated and measured reflection coefficient plot of proposed antenna
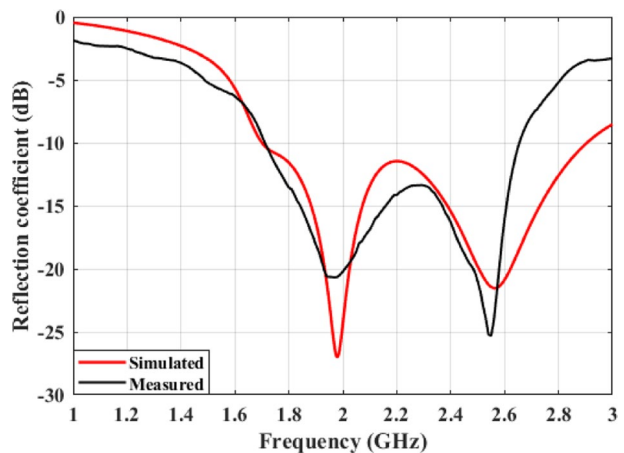
Table 2 Simulated and measured results comparison

Parameters	Simulated	Measured
Impedance bandwidth (%)	53.04 (1220 MHz)	43.12 (940 MHz)
Band range (GHz)	1.69–2.91	1.71–2.65
Resonant frequency (GHz)	1.98, 2.56	1.97, 2.55
Reflection coefficient (dB)	− 27.14, − 21.49	− 20.65, − 25.29
Gain (dB)	3.84, 3.47	3.7, 3.3
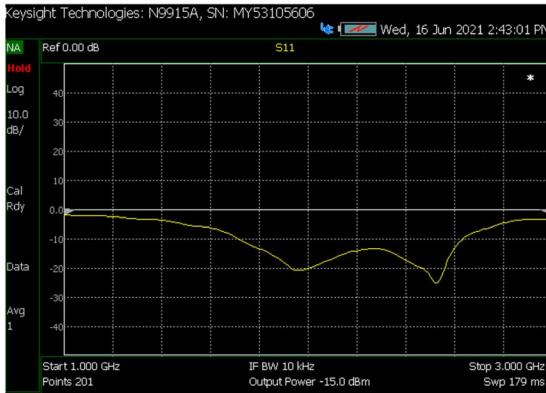
Fig. 12 **a** Photograph of measured reflection coefficient **b** Photograph of measurement setup

chamber. The pattern is bi-directional in the E-plane, with peak gains (simulated) of 3.73 dB for the major lobe and 2.83 dB for the back lobe at frequency 1.98 GHz while it is 3.36 dB for the major lobe and 3.1 dB for the back lobe at frequency 2.56 GHz. The proposed antenna has 3 dB beamwidth of 50.4° (78.5°, 128.9°) at frequency 1.98 GHz and 73.4° (65.9°, 139.3°) at frequency 2.56 GHz. The simulated and measured peak gain plot of proposed antenna is shown in Fig. 14. The stable peak gains of 3.84 dB and 3.47 dB for simulated antenna while peak gains of 3.7 dB and 3.3 dB for measured antenna is obtained at frequencies 1.98 GHz and 2.56 GHz respectively. The simulated directivity of 3.4 dB and 3.5 dB while antenna efficiency of 90.7% and 90.3% are obtained at frequencies 1.98 GHz and 2.56 GHz as shown in Fig. 15.

The performance comparison of proposed antenna design with reference antennas reported in [11–20] in terms of overall size, resonant frequency, operating range, impedance bandwidth, gain and applications are shown in Table 3. It is clearly observed from Table 3 that the proposed antenna is more compact with overall size (1797 mm^2) and wide bandwidth of 53.04% (1220 MHz) compared to all reported antennas [11–20] of single band. In reported antennas of Table 3, only antenna [19] (1920 mm^2) has overall size near to proposed antenna (1797 mm^2) whereas antennas [12] (3456 mm^2) and [20] (3600 mm^2) have comparatively large size with factor of 1.92 and 2.01 respectively. Reference antennas [11] (6050 mm^2), [13] (5456 mm^2) and [15] (5898 mm^2) also have large size with factor of 3.67, 3.04 and 3.28 respectively. However, [14] (9600 mm^2), [16] (11236 mm^2), [17] (10,000 mm^2) and [18] (7744
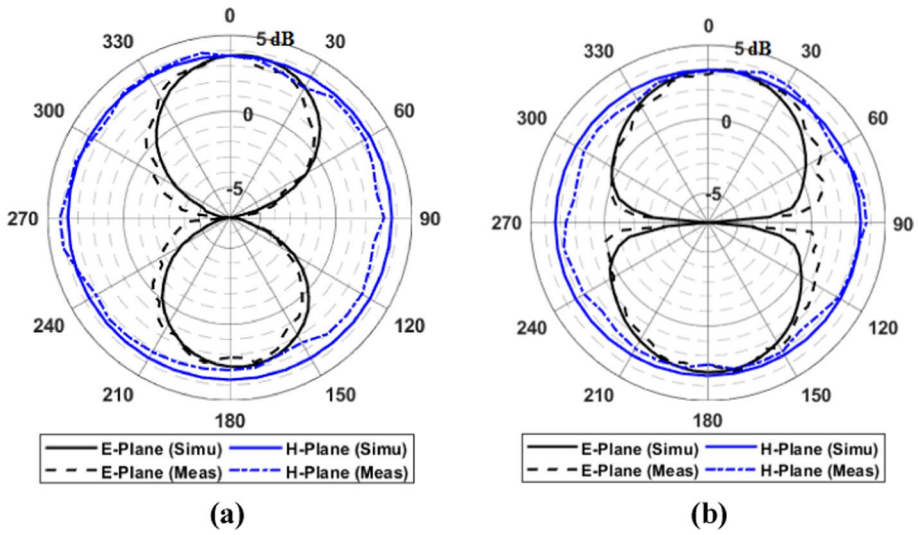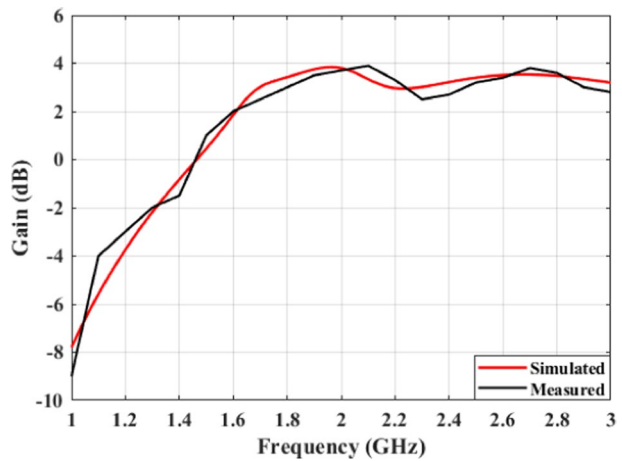
Fig. 13 E and H-plane radiation pattern (simulated and measured) of antenna at frequency **a** 1.98 GHz **b** 2.56 GHz

Fig. 14 Gain graph of proposed antenna (simulated and measured)

mm^2) have large size with large factor of 5.34, 6.25, 5.56 and 4.31 respectively. The impedance bandwidth (1220 MHz) of proposed antenna is wider than [12] (970 MHz),

Fig. 15 Directivity and efficiency graph (simulated) of proposed antenna
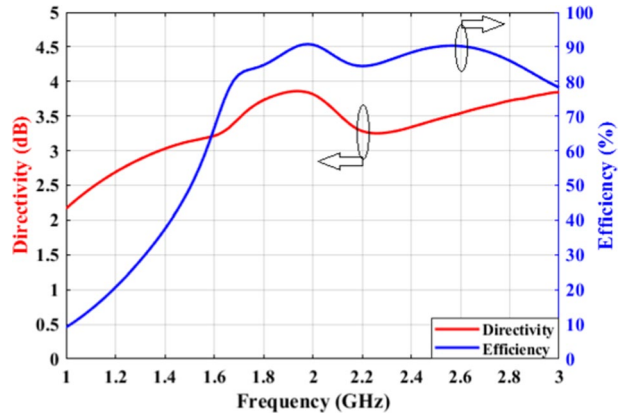
[13] (990 MHz), [16] (1070 MHz), [19] (1120 MHz) and [20] (1030 MHz) with difference of 250 MHz, 230 MHz, 150 MHz, 100 MHz and 190 MHz whereas large difference of 930 MHz, 660 MHz, 800 MHz, 720 MHz and 570 MHz with [11] (290 MHz), [14] (560 MHz), [15] (420 MHz), [17] (500 MHz) and [18] (650 MHz) is observed respectively. Thus, the proposed antenna is not only compact in size but also have larger bandwidth.

8 Conclusion

A simple and small size microstrip antenna is designed and modelled to circumvent the limitation of narrow bandwidth of conventional antenna and experimentally confirmed. The bandwidth of proposed antenna is increased upto 53.04% (1220 MHz) between 1.69 and 2.91 GHz resonating at two frequencies 1.98 GHz and 2.56 GHz with − 27.14 dB and − 21.49 dB reflection coefficient. The value of VSWR at the resonance frequency 1.98 GHz and 2.56 GHz is 1.09 and 1.18, which is much closer to the ideal value of l.0. There is good agreement between the simulation and measured results. Because of its tiny size and simple structure, it can be employed for low-cost wireless applications. PCS (1.85–1.99 GHz), UMTS (1.92–2.17 GHz), WLAN (2.4–2.484 GHz), and WiMAX (2.5–2.69 GHz) applications can all be employed in the same frequency spectrum 1.69–2.91 GHz. In the whole resonant band, a consistent peak gain of 2.9–3.84 dB and antenna efficiency of 81–91% is found.

Table 3 Comparison between proposed and reported reference antennas [11–20]

Refs.	Overall size (mm^2)	Resonant Freq.(GHz)	Operating range (GHz)	Impedance bandwidth (%)	Gain (dB)	Applications
[11]	55 × 110 = 6050	0.89/1.16	0.88–1.17	28 (290 MHz)	7	GSM
[12]	54 × 64 = 3456	1.975	1.49–2.46	49 (970 MHz)	3.4	GSM/WiMAX/ WLAN
[13]	88 × 62 = 5456	3.0	2.38–3.36	36.5 (990 MHz)	NR	WLAN/WiMAX
[14]	120 × 80 = 9600	1.84	1.56–2.12	30.5 (560 MHz)	9.8	Broadband
[15]	76.8 × 76.8 = 5898	1.3	1.09–1.51	32.1 (420 MHz)	5	Broadband
[16]	106 × 106 = 11,236	1.7/2.3/2.7	1.68–2.75	48 (1070 MHz)	8.9	2G/3G/4G
[17]	100 × 100 = 10,000	NR	1.1–1.6	32 (500 MHz)	NA	GNSS
[18]	88 × 88 = 7744	2.45	2.29–2.94	24.8 (650 MHz)	3	WLAN/WiMAX
[19]	40 × 48 = 1920	2.73	2.23–3.35	41 (1120 MHz)	3.6	WLAN/WiMAX
[20]	60 × 60 = 3600	2.56	2.32–3.35	40.23 (1030 MHz)	8.2	WLAN/WiMAX
Proposed	38.4 × 46.8 = 1797	1.98, 2.56	1.69–2.91	53.04 (1220 MHz)	3.84	PCS/UMTS/WLAN/WiMAX

NR: Not reported (Value is not given in article)

Data Availability Data sharing not applicable to this article as no datasets were generated or analysed during the current study.

Declarations

Conflict of interest The author declares no potential conflict of interest.

References

1. Pozar, D. M. (1992). Microstrip antennas. *Proceeding of the IEEE, 80*(1), 79–91.
2. Balanis, C. A. (2005). *Antenna theory, analysis and design*. New Jersey: Wiley.
3. Liu, N., Zhu, L., & Choi, W. (2017). A differential-fed microstrip patch antenna with bandwidth enhancement under operation of TM10 and TM30 modes. *IEEE Transactions on Antennas and Propagation, 65*(4), 1607–1614.
4. Gangwar, S. P., Gangwar, K., & Kumar, A. (2018). A compact modified hexagonal slot antenna for wideband applications. *Electromagnetics, 38*(6), 339–351.
5. Gupta, N., Saxena, J., & Bhatia, K. S. (2020). Optimized metamaterial-loaded fractal antenna using modified hybrid BF-PSO algorithm. *Neural Computing and Applications, 32*, 7153–7169.
6. Geetharamani, G., & Aathmanesan, T. (2020). Design of metamaterial antenna for 2.4 GHz WiFi applications. *Wireless Personal Communications, 113*, 2289–2300.
7. Cheng, W. E., & Yao, S. L. (2014). An improved wideband dipole antenna for global navigation satellite system. *IEEE Antennas and Wireless Propagation Letters, 13*, 1305–1308.
8. Verma, R. K., & Srivastava, D. K. (2019). Design, optimization and comparative analysis of T-shape slot loaded microstrip patch antenna using PSO. *Photonic Network Communications, 38*(3), 343–355.
9. Verma, R. K., & Srivastava, D. K. (2021). Optimization and parametric analysis of slotted microstrip antenna using particle swarm optimization and curve fitting. *International Journal of Circuit Theory and Applications, 49*(7), 1868–1883.
10. Gupta, A., & Chaudhary, R. (2017). A compact CPW-fed wideband metamaterial-inspired antenna for GSM, WLAN/Wi-Fi, and WiMAX applications. *International Journal of Microwave and Wireless Technologies, 9*(3), 567–571.
11. Deshmukh, A. A., & Ray, K. P. (2013). Analysis of L-shaped slot cut broadband rectangular microstrip antenna. *International Journal of Electronics, 100*(8), 1108–1117.
12. Gupta, N., Saxena, J., & Bhatia, K. S. (2019). Design of wideband flower-shaped microstrip patch antenna for portable applications. *Wireless Personal Communications, 109*, 17–30.
13. Ansari, J. A., Yadav, N. P., Singh, P., & Mishra, A. (2010). Analysis of broadband operation of disk patch antenna with parasitic elements in single and two layer structures. *International Journal of Microwave and Optical Technology, 5*(3), 140–147.
14. Kamakshi, K., Singh, A., Aneesh, M., & Ansari, J. A. (2014). Novel design of microstrip antenna with improved bandwidth. *International Journal of Microwave Science and Technology*. https://doi.org/10.1155/2014/659592
15. He, M., Ye, X., Zhou, P., Zhao, G., Zhang, C., & Sun, H. (2015). A small-size dual-feed broadband circularly polarized U-slot patch antenna. *IEEE Antennas and Wireless Propagation Letters, 14*, 898–901.
16. Zhou, Z., Wei, Z., Tang, Z., & Yin, Y. (2019). Design and analysis of a wideband multiple microstrip dipole antenna with high isolation. *IEEE Antennas and Wireless Propagation Letters, 18*(4), 722–726.
17. Sun, C., Wu, Z., & Bai, B. (2017). A novel compact wideband patch antenna for GNSS application. *IEEE Transactions on Antennas and Propagation, 65*(12), 7334–7339.
18. Zhang, J., Lu, W. J., Li, L., Zhu, L., & Zhu, H. B. (2016). Wideband dual-mode planar endfire antenna with circular polarization. *Electronics Letters, 52*(12), 1000–1001.
19. Bala, B. D., Rahim, M. K. A., & Murad, N. A. (2015). Bandwidth enhancement metamaterial antenna based on transmission line approach. *Microwave and Optical Technology Letters, 57*(1), 252–256.
20. Sharma, A. K., Mittal, A., & Reddy, B. V. R. (2015). Asymmetrical π-shaped slot embedded microstrip antenna for circular polarization. *Wireless Personal Communications, 83*, 2069–2083.
21. Chaturvedi, D., & Raghavan, S. (2019). A compact metamaterial-inspired antenna for WBAN application. *Wireless Personal Communications, 105*, 1449–1460.

22. Dwivedi, A. K., Sharma, A., Pandey, A. K., & Singh, V. (2021). Two port circularly polarized MIMO antenna design and investigation for 5G communication systems. *Wireless Personal Communications, 120*, 2085–2099.
23. Rao, Q., & Denidni, T. A. (2007). Ultra-wideband and uni-directional radiation slot antenna for multi-band wireless communication applications. *Wireless Personal Communications, 41*, 507–516.
24. Gangwar, A., & Alam, M. S. (2017). A high FoM monopole antenna with asymmetrical L-slots for WiMAX and WLAN applications. *Microwave and Optical Technology Letters, 60*, 196–202.
25. Zeland Software Inc. 'IE3D' electromagnetic simulation and optimization package, Version 14
26. Verma, R. K., & Srivastava, D. K. (2020). Design and analysis of triple-band rectangular microstrip antenna loaded with notches and slots for wireless applications. *Wireless Personal Communications, 114*, 1847–1864.

Ramesh Kumar Verma is born on 15, June 1985 in Ambedkar Nagar, Uttar Pradesh India. He is currently pursuing Ph.D from AKTU Lucknow, Uttar Pradesh India. He had completed M.Tech in year 2015 from Bundelkhand Institute of Engineering and Technology Jhansi, in Digital communication. He had completed B. Tech in year 2009 from Raj Kumar Goel Institute of Technology Ghaziabad in Electronics and Communication Engineering. He is an expert in antenna designing, fabrication, IE3D simulation software and Particle Swarm Optimization (PSO) Algorithm. Presently he is working on optimization of microstrip patch antenna with PSO and curve fitting.